Available online at www.sciencedirect.com
SCIENCE DIRECT®
Thermochimica Acta 426 (2005) 23–31
thermochimica acta
www.elsevier.com/locate/tca

A generalisation of the non-parametric, NPK (SVD) kinetic analysis method Part 2. Non-isothermal experiments

G. Roger Heal*

Department of Chemistry, University of Salford, Salford M5 4WT, UK

Received 6 April 2004; received in revised form 26 June 2004; accepted 6 July 2004
Available online 14 August 2004

Abstract

The non-parametric method of kinetic analysis using singular value decomposition of a matrix of data values, as proposed by Nomen and Sempere, is applied to differential and integral analysis of non-isothermal results. It is demonstrated again that a correction has to be applied to obtain the correct value of the pre-exponential constant *A*, as in Part 1 of this series. The two methods are tested using simulated data and show very accurate retrieval of the starting values of activation energy and pre-exponential constants. A set of data for the decomposition of calcite under vacuum, treated non-isothermally, was taken from the ICTAC study of kinetic methods. The results obtained agree reasonably with those reported from the study.

Keywords: Kinetic analysis; Non-parametric; Singular value decomposition; SVD; Non-isothermal; Simulated data; Calcite

1. Introduction

Following the study of isothermal experiments in Part 1, a similar treatment is now given to non-isothermal experiments analysed by differential and integral methods. Simulated and experimental data was analysed using computer programs developed from these methods. The results for non-isothermal experiments are shown in Table 1.

2. Non-isothermal experiments—differential analysis

2.1. Applying SVD

Singular value decomposition of data arrays was applied in the same manner as described in the previous papers on this subject [1–5] and reported in Part 1. The basic equations from Part 1 still apply, but allowance now has to be made for the rising temperature, which leads the some terms having different meanings.

The difficulty in analysis arises because the data covers α from 0 to 1 and a wide temperature range. Because of the nature of the experiment, the whole α range is not available over all of the temperature range. The solution followed is as in the previous studies [1–5]. The total range of data was divided up into submatrices, each enclosing a range of temperatures and α values covered by the experimental conditions. These submatrices **S** of experimental data were then analysed separately by the SVD procedure. This gave several sets of **U**, **W** and **V** matrices. As before, only the first columns were required from **U** and **V** and were designated **u** and **v**. Also only **W**(1) was of any significance and was designated **w**. The sets of values of **u** and **v** were then combined into one set by adding the second and subsequent sets to the first, after multiplying by suitable constants. To enable this, at least one line of data must be common between successive blocks. Sempere et al. [1–4] used this amount of overlap of one line between sets. In the present study a greater overlap was used.

* Present address: 4 Hazelbadge Close, Poynton, Stockport SK12 1HD, UK. Tel.: +44 1625 874850; fax: +44 1625 874850.
E-mail address: roger_heal@yahoo.com (G.R. Heal).

0040-6031/$ – see front matter © 2004 Elsevier B.V. All rights reserved.
doi:10.1016/j.tca.2004.07.003

Table 1
Non-isothermal experiments

Sample	Starting simulation values		Analysis results				Isoconversional method	
	Input E (kJ/mol)	Input A (s^{-1})	Average E (kJ/mol)	Standard deviation in E (kJ/mol)	Overall E (kJ/mol)	A (s^{-1})	E (kJ/mol)	A (s^{-1})
Differential analysis								
Simulated A2	130.0	1.0×10^{13}	130.007	0.188	130.011	1.009×10^{13}	130.001	1.008×10^{13}
Simulated A3	120.0	1.0×10^{12}	120.017	0.075	120.011	1.003×10^{12}	119.972	0.996×10^{12}
Calcite in vacuum								
Overall	–	–	104.7	9.2	105.6	3.31×10^{7}	105.8	2.57×10^{8}
Low α			130.5					
High α			109.5					
Integral analysis								
Simulated A2	130.0	1.0×10^{13}	129.996	0.007	129.994	0.997×10^{13}	As above	As above
Simulated A3	120.0	1.0×10^{12}	120.009	0.037	120.020	1.005×10^{12}	As Above	As Above
Calcite in vacuum								
Overall	–	–	125.0	13.9	127.8	5.19×10^{8}	As Above	As Above
Low α			170.5					
High α			109.3					

Table of activation energies and pre-exponential factors found by analysis using SVD and isoconversional Arrhenius plot. The results from the simulated data are given to more significant figures than would normally be justified to indicate the precision of the retrieval of the starting figures.

The second submatrix of data overlapped the first submatrix by all of the lines, except for the first line of submatrix $\mathbf{S}_1$ and the last line of submatrix $\mathbf{S}_2$.

2.2. Interpolation along the data curves

Before choosing the position of these blocks of data, interpolation was carried out on the experimental data. First interpolation was taken along each data set at one heating rate. A step size of 0.01 for α did not always lead to consistent submatrices, that is, covering the required width of temperature and overlapping with other submatrices. It was found to be better to use smaller steps of α of 0.005 from 0.1 to 0.95. For the lower region below $\alpha = 0.1$ and above $\alpha = 0.95$ a step size of 0.001 was used. Interpolation was carried out along the original data curves to give the temperatures T_e at which these values of α were produced. At the same time the gradients $(d\alpha/dT)_e$ were calculated and stored for the same point on the curves. These gradients were multiplied by the heating rate β in $K\,s^{-1}$ for the particular experiment. This converted the gradients to $(d\alpha/dt)_e$. As in Part 1, either a cubic fit with a quadratic fit at the top end was used, or a polynomial equation with variable degree and number of points.

2.3. Interpolation across the data

It is assumed that the total set of curves fit together to give a two-dimensional data surface. The independent variables are temperature and α. The dependant variable is gradient $(d\alpha/dt)_e$. Taking lines across the surface at constant α values, a second interpolation was then made. A step in temperature of ΔT was chosen and a starting value of T_i. To get the starting T_i, the first T_e value on that line was rounded up to the nearest multiple of ΔT. Steps of T_i were then taken across the line and stopped when the next T_i would exceeded the last experimental T_e on that line. The quantity ΔT could be set during the calculation and was chosen so that, considering the temperature ranges across one line, the number of T_i values produced was 20–30. The number used sometimes had to be adjusted to other values to get correct overlap of the submatrices. Interpolation was then carried out to obtain new values of gradient at these T_i points. The new data across a line could also be used in an isoconversional calculation, because it should fit an Arrhenius plot. Therefore, before the interpolation, the logs of the gradients were taken and the reciprocal of the T_e values. These quantities should fit a straight line. In case the fit was not exact, a quadratic equation was also tested for the interpolation. However, the results were not as good as for the linear equation, because small fluctuations were exaggerated to give a poor fit. The coefficients of the linear equation were used to get an interpolated value at $1/T_i$ points and the antilog taken to obtain a new gradient $(d\alpha/dt)_i$. The gradient of the linear fit was also used to obtain a value of isoconversional activation energy. As well as ΔT, the width of the data set in the submatrix, *n*range, could be chosen, as could the number of lines in the submatrix, *n*lines. If this were too high, then there would be insufficient data across each line to fill the submatrix to produce a continuous set. If it were too low the results from each submatrix would be inaccurate. Trial and error had to be used to select ΔT, *n*range and *n*lines. The interpolated values of $(d\alpha/dt)_i$ corresponded to $\mathbf{M}$ in Eq. (6) of Part 1 and were a function of T_i and α. This matrix of values was then used in the SVD calculation, within each submatrix. The decomposition of $\mathbf{M}$ into two functions without prior knowledge of the functions applies exactly as in Part 1, Section 2.1. As the steps of α progressed up the curves, this gave a complete set of E values, which could be examined to see if any change in mechanism was appearing. A minimum of *n*lines = 5 lines was used. At the ends of the data set, where α is low or high, the experimental

curves run nearer to horizontal. In these regions it is not possible to choose submatrices that overlap correctly. The "adaptive NPK method" used in Refs. [1–5] was used in that the height of the submatrix, *n*lines, was reduced in this region to three lines only. For clarity in presentation, only the values of activation energy and pre-exponential constant are shown at intervals of α of 0.01. If the end regions were important the results from the full set of α could be output. A listing of the individual E values from each submatrix was made, so that they could be examined for scattered values at the ends. Provision was made to exclude these points, leading to a restricted range of α values as is shown in results in subsequent plots.

To make up a complete set of values of **u** and **v** to use over the whole range of the experiment, a scaling procedure had to be used as explained in the previous papers [1–5]. The first set of **u** and **v** were left as calculated from the first submatrix $\mathbf{S}_1$. The second value in **u** from data submatrix $\mathbf{S}_1$, $(\mathbf{u}_2)_{s1}$, and the first value from the submatrix $\mathbf{S}_2$, $(\mathbf{u}_1)_{s2}$, was used to calculate a correction factor a_2:

$$a_2 = \frac{(\mathbf{u}_2)_{s1}}{(\mathbf{u}_1)_{s2}} \tag{1}$$

Then a_2 was used to correct the scale of all the remaining values in $(\mathbf{u})_{s2}$ so that the results joined up with those from the first submatrix

$$\text{rescaled}(\mathbf{u}_i)_{s2} = a_2 \cdot (\mathbf{u}_i)_{s2}, \quad i = 2, n \tag{2}$$

where n is the number of lines of data in a submatrix. For the first submatrix it is implied that the correction is applied with $a_1 = 1$.

This was repeated for each submatrix data set, obtaining a new a_i value each time. The rescaled values of $\mathbf{u}_i$ from all of the submatrices were then combined into one vector $\mathbf{u}_T$. The **v** vector quantities also require scaling and at the same time multiplying by the value of **w** for the particular submatrix. The same values of a_i may be used because:

$$\text{rescaled}(\mathbf{v}_i)_{s2} = \frac{(\mathbf{v}_i)_{s2}}{a_2} \cdot (w)_{s2}, \quad i = 2, n \tag{3}$$

The correction of the values for the first submatrix is included, i.e. multiplying by $(\mathbf{w})_{s1}$ and dividing by $a_1 = 1$. The **v** values are combined into a continuous set $\mathbf{v}_T$. In Eq. (2) of Part 1 temperature T varies continuously with time t in one experiment. However, the generation of the total set of $\mathbf{u}_T$ and $\mathbf{v}_T$ values is equivalent to a data surface with axes T and α and thus in Eq. (3) of Part 1, $h(T)$ is equivalent to the total $\mathbf{v}_T$ vector and $f(\alpha)$ was equivalent to total $\mathbf{u}_T$. The log of the total set of $\mathbf{v}_T$ values was plotted against $1/T$ in an Arrhenius plot. Any deviation from a straight line was noted as a possible change in mechanism. The gradient yielded an overall value of E. As in Part 1, the values in $\mathbf{u}_T$ were plotted against α to check against standard curves to determine the mechanism being obeyed. Finally the intercept was corrected as in Eqs. (8) and (9) of Part 1, Section 2.2.1.

3. Non-isothermal experiments—integral analysis

3.1. Applying SVD

Before integrating Eq. (2) of Part 1, time t has to be replaced by temperature T using the equation:

$$\mathrm{d}T = \beta \, \mathrm{d}t \tag{4}$$

where β is the heating rate in $\mathrm{K\,s^{-1}}$.

The new equation may now be integrated:

$$\int \frac{\mathrm{d}\alpha}{f(\alpha)} = \int \frac{A}{\beta} \mathrm{e}^{-E/RT} \, \mathrm{d}T \tag{5}$$

The left-hand side produces $g(\alpha)$ the integral rate equation. On the right-hand side, the substitution X=E/RT is usually made. In several steps this reduces the equation to:

$$g(\alpha) = \frac{AE}{R\beta} \int_{X_0}^{X} \mathrm{e}^{-X} X^{-2} \, \mathrm{d}X \tag{6}$$

where X_0 is the value of X at the start of the experiment. The integral cannot be determined analytically but is usually written:

$$p(X) = \int_{X_0}^{X} \mathrm{e}^{-X} \, X^{-2} \, \mathrm{d}X \tag{7}$$

so

$$g(\alpha) = \frac{AE}{R\beta} p(X) = \frac{AE}{R\beta} p\left(\frac{E}{RT}\right) \tag{8}$$

In a set of non-isothermal experiments, at various heating rates, the experimental quantities are α, T and β. These could be separated from Eq. (8) to form:

$$\beta = \frac{1}{g(\alpha)} \frac{AE}{R} p(X) \tag{9}$$

Comparison with Eq. (6) of Part 1 shows that $\boldsymbol{\beta}$ is now an array of values corresponding to **M**. The spatial representation of the set of experiments is a surface of values of $(\mathrm{d}\alpha/\mathrm{d}t)_e$ with axes T_e and α, but can equally well be represented as a surface of values of $\boldsymbol{\beta}$ with axes of T_e and α. The interpolation across the surface for a single α value may then be made, using as data the set of experimental β values and the experimental T_e values. Trials were made of various interpolation equations. The best fit was still taking the log of the dependent variable β and the reciprocal of the independent variable T_e. A good linear fit was produced with this data, but a quadratic fit was marginally better and so was adopted. This interpolation for constant T_i values produced β_i. There is, of course, no experimental meaning to values of β_i, but there is no mathematical reason why they should not be used. They could be defined as the heating rate at which the sample would have had to be heated to achieve a particular α value,

at a particular temperature. Comparing Eq. (9) and Eqs. (3) and (6) of Part 1, $f(\alpha)$ is replaced by $1/g(\alpha)$ and $h(T)$ by

$$h(T) = \frac{AE}{R} p(X) = \mathbf{v} \tag{10}$$

The **u** vector contains a set of $1/g(\alpha)$ values and **v** contains a set of values of $(AE/R)p(X)$, one for each temperature T. Although the Arrhenius equation is invoked to enable the function $\mathbf{v} = (AE/R)p(X)$ to be obtained, the matrix of **β** values may still be resolved into **u** and **v** without prior knowledge of these functions. Therefore the method is still NPK in nature.

The next problem is that $p(X)$ cannot be found by integration. There are, however, approximation equations for its value, of varying precision, which are reviewed in Refs. [7,8]. The most precise set of values is probably given by Chebyshev polynomials [7]. The precision of the value of $p(X)$ may be increased, at the expense of speed, by using more terms in the equation, as explained in Ref. [7]. In this application, a reasonable compromise for the number of terms used was 15 and that seemed to produce good enough agreement for the simulated data. However, a higher number of terms would be required if $p(X)$ had to be evaluated with low values of X, i.e. a low value of E and high temperature.

The calculations were first applied to the subset of data in each submatrix alone. Since the Chebyshev polynomials give the value of $p(X)$ for input values of E and T, and Eq. (10) contained E and A in the first term, iterative methods had to be devised. These consisted of an inner and an outer iteration. The section of the computer program dealing with this is represented by a flow diagram in Fig. 1. For the outer iteration, standard starting values of E and A were used, namely $E = 100{,}000\ \mathrm{J\,mol^{-1}}$ and $A = 10^{10}\ \mathrm{s^{-1}}$, respectively, with the experimental temperatures T_i. These were used to calculate AE/R. Eq. (10) was transposed and used with the experimental results held in **v** to obtain experimental values of $p_e(X)$

$$p_e(X) = \frac{h(T)}{AE/R} = \frac{\mathbf{v}}{AE/R} \tag{11}$$

Each temperature T_i was used in turn and with a single value extracted from the vector **v**. The quantity X_T was given the nominal value of 30 and $p(X_T)$ was calculated by Chebyshev polynomials. The value of $p(X_T)$ was compared with $p_e(X)$ from Eq. (11), for one temperature T_i. X_T was adjusted up or down in steadily decreasing steps, in the inner iteration, until the two p values agreed to better than 10^{-12}. The final value of X_T was then the value of X to fit Eq. (11). The procedure was repeated for the other temperatures in the set. Since $X_T = E/RT_i$, a plot could then be made of X_T against $1/T_i$ and the gradient was E/R. This is not an Arrhenius plot so the gradient is positive, not negative, here. The value of E obtained then became the new value of E for the next step of the outer iteration. This new value of E was then also used at each temperature T_i to obtain values $X_i = E/RT_i$ and thus $p(X_i)$ by Chebyshev polynomials again. Transposing Eq. (10) another

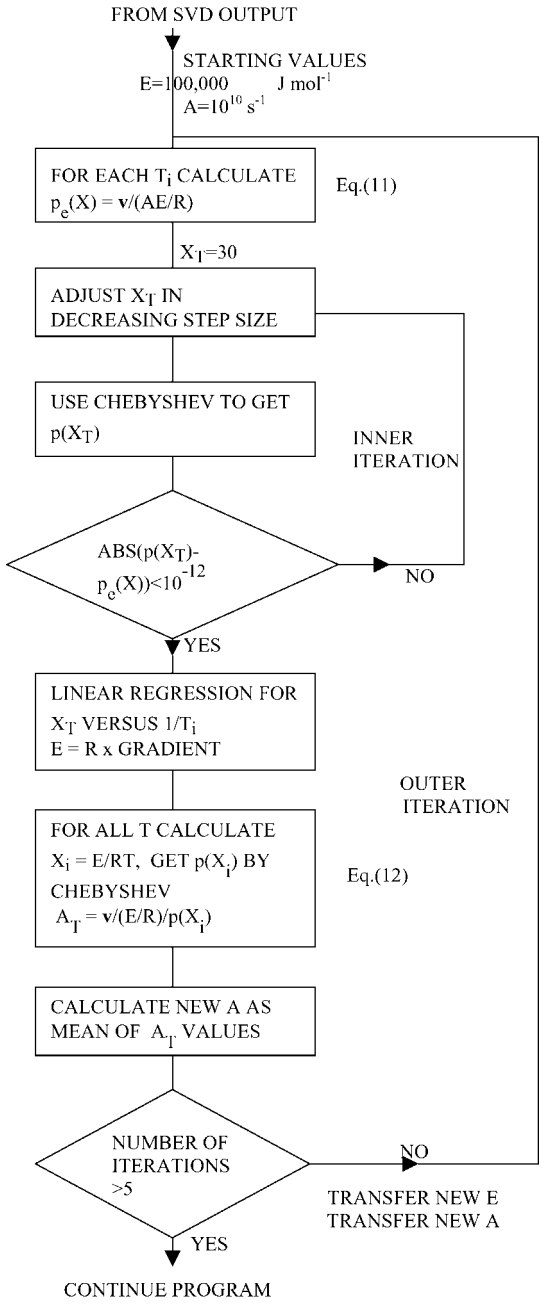

Fig. 1. Flow diagram covering part of the computer program dealing with the iterative determination of E and A in the case of non-isothermal data with integral analysis.

way gives:

$$A_T = \frac{\mathbf{v}}{(E/R)p(X_i)} \tag{12}$$

This produced new values of A_T for each temperature. The mean of these values gave a new value of A for the outer iteration. The outer iteration was now repeated with the new E and A, again using the inner iteration to adjust X_T to match $p(X_T)$ to $p_e(X)$. In practice only five loops of the outer iteration were required to produce convergence to constant values of

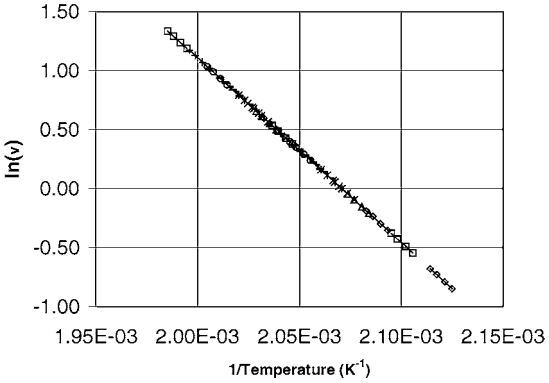

Fig. 2. Differential analysis of non-isothermal data. Arrhenius plot of ln(**v**), i.e. ln(rate) vs. $1/T$ for simulated data for mechanism A2, i.e. Eq. (13) of Part 1. The individual plots for the submatrices are superimposed, but only the first and last and two intermediate points are shown for each. Also only every fifth submatrix line is shown for clarity. Various symbols are used for each submatrix.

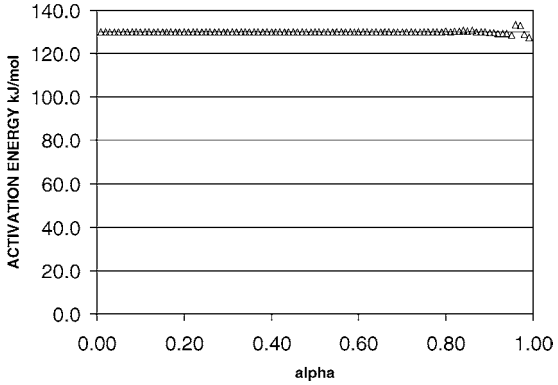

Fig. 3. Variation of activation energy with α for non-isothermal data. Comparison of differential and integral analysis. Simulated data for mechanism A2, i.e. Eq. (13) of Part 1. (△) Differential analysis, (—) integral analysis.

E and A. These final values of E and A were then the result of the SVD method.

The calculation was repeated for the other submatrices of data. The individual values of E and A were output to see if there were any changes of mechanism. Also the mean values of E and A were determined. The data produced in the individual vectors $\mathbf{u}_i$ and $\mathbf{v}_i$ from the submatrices could also be combined into one set using scaling factors $\mathbf{a}_i$ and $\mathbf{b}_i$ as explained for differential analysis above. The quantity $\mathbf{v}_T$ was then used as $\mathbf{v}$ in Eqs. (10) and (11). The iteration procedures were then repeated over the whole data set. This gave single overall values of E and A. These quantities are of limited significance if the mechanism has changed during the reaction. The reciprocal of the result in vector $\mathbf{u}_T$ was used as $g(\alpha)$ to match to theoretical equations by a plot of each theoretical, rescaled $g_t(\alpha)$ against α to determine the mechanism.

The value of A obtained in these calculation required correction, after the $g(\alpha)$ equation that fits had been determined, as explained in Section 2.2 of Part 1 for integral isothermal data.

4. Testing with simulated data

A second computer program was written in Fortran77, this time to carry out the analysis of the non-isothermal data.

4.1. Non-isothermal data by a differential analysis

Non-isothermal simulated data for mechanism A2, Eq. (13) of Part 1, was generated with the same starting values of E and A as above, using heating rates of 1.0, 1.1, 1.2, 1.3 and 1.4 K s^{-1}. The value of ΔT chosen was 0.1 K and the width of the submatrix (*n*range) was 25. The height of the submatrix (*n*lines) was 5. Fig. 2 shows the superimposed Arrhenius plots, obtained from the separate submatrices, and is almost a perfect straight line. Fig. 3 shows the variation in E obtained from these individual SVD analyses. A slight fluctuation in E is shown at the highest α values. This is presumably due to the inaccuracies of the smoothing/differentiation technique. Attempts were made to improve this region, using other curve-fitting techniques, but the fluctuations could not be removed. The mean value of these E values was obtained. Data from a selected range of α values were combined as a single SVD calculation and plotted in Fig. 4, leading to an overall activation energy. The plot of $f(\alpha)$ versus α for the experimental points, compared with the theoretical equation, was the same as Fig. 3, Part 1, for the isothermal data, with the same degree of fit. However, the ordinate scale was different. Clearly Eq. (13) of Part 1 is the correct fit. A corrected value of A could then be obtained. Also, the isoconversional results across the data surface at each α value were used for individual Arrhenius plots.

The analysis was repeated using the equation tested by Sewry and Brown [5]. This was equation A3 (mechanism 15 of Ref. [12] in Part 1), in the usual nomenclature:

$$\frac{d\alpha}{dt} = A\, e^{-E/RT}(1-\alpha)[-\ln(1-\alpha)]^{2/3} \quad (13)$$

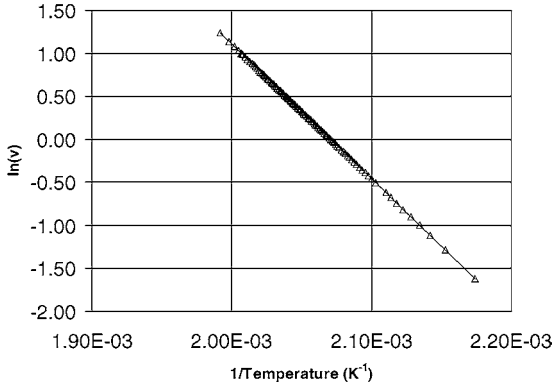

Fig. 4. Differential analysis of non-isothermal data. Arrhenius plot of ln(**v**), i.e. ln(rate) vs. $1/T$ for simulated data for mechanism A2, i.e. Eq. (13) of Part 1. The plot is for the total data after combining all of the **v** values from the submatrices. Only every fifth point is shown for clarity.

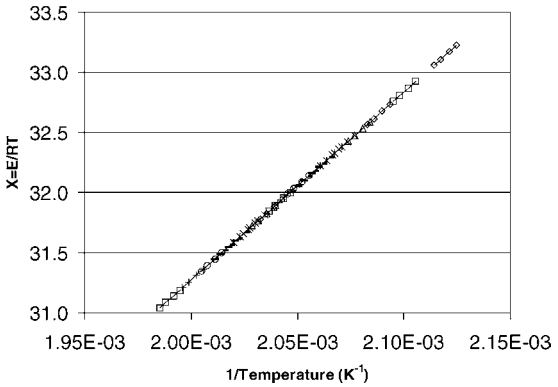

Fig. 5. Integral analysis of non-isothermal data. Simulated data for mechanism A2, i.e. Eq. (13) of Part 1. Superimposed $X = E/RT$ vs. $1/T$ plots for individual submatrices. Only the first and last and two intermediate points are shown for each submatrix. Also only every fifth submatrix is shown for clarity. Various symbols are used for each submatrix.

The values of E and A used in the simulation were as in Ref. [5], i.e. 120 kJ/mol and 1.0×10^{12} s^{-1} with heating rates of 1, 2, 5, 10 and 20 K min^{-1}. The value of ΔT chosen was 0.1 K, *n*range was 15 and *n*lines was 5. The analysis was carried in the same manner as for the A2 data above and the results also shown in Table 1. The value of A is much closer to the simulation starting value than that obtained by Sewry and Brown, presumably because of the correction here applied to the intercept.

4.2. Non-isothermal data by an integral analysis

In this analysis X has to be plotted against $1/T$ and this is shown in Fig. 5 for the whole set of submatrices and a mean value of E determined. The data in a selected range was then put into the iteration calculation. Only a small number of outer iterations are required, which is shown in Fig. 6 by the fact that only the points of the first two lines are separate, the points on subsequent lines appear to be coincident. The gradient of Fig. 6 yielded an overall E value. The plot of $g(\alpha)$ against α for experimental and theoretical data was the same as Fig. 5 for isothermal data in Part 1 and shows Eq. (13) of Part 1 fitted as expected. Again the ordinate scale was different. The corrected value of A could then be found. The variation of E with α for this method is also shown in Fig. 3 and shows no variation at the high α end, unlike the differential method. The isoconversional results are the same as for the differential method.

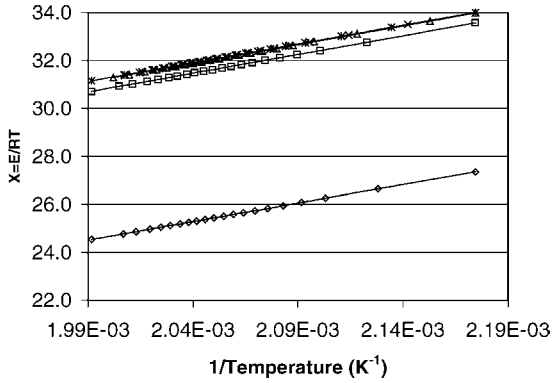

Fig. 6. Integral analysis of non-isothermal data. Simulated data for mechanism A2, i.e. Eq. (13) of Part 1. Combined **v** results from all of the submatrices used in the iterative process. (◊) First step of the iteration, (□) second step of the iteration, (△) third step of the iteration, (×) fourth step of the iteration, (*) fifth step of the iteration. The upper line shows superimposed symbols showing rapid convergence to the final line. Not all of the symbols are drawn at each $1/T$ point to make the plot clearer.

5. Testing with experimental data

5.1. Non-isothermal data by a differential analysis

The method was applied to the data from the ICTAC kinetic study [6]. The non-isothermal data used was for the decomposition of calcite in vacuum (called CCVKPM.TXT). The heating rates were 1.8, 2.5, 3.5, 5.0, 6.2 and 10 K min^{-1}. For this analysis, trials proved that a ΔT of 2 K was suitable. The best *n*range value was 20 and the *n*lines chosen was again 5. The individual Arrhenius plots are shown in Fig. 7. From the gradients of these plots the variation of E with α is obtained and shown in Fig. 8. If the submatrix data is combined, the resulting single plot is shown in Fig. 9. An attempt to fit an equation in the $f(\alpha)$ versus α plot in Fig. 10 was difficult because of the fluctuations in the plot. The nearest equation showing the general shape was A2 (mechanism 14 from Ref. [12], Eq. (13) from Part 1). The individual Arrhenius plots for the isoconversional data were also made. Because of the variation in E across the whole α range, the method was also applied over two very restricted α ranges, from 0.0 to 0.1 and 0.9 to 1.0. These results appear in Table 1 as low α and high α.

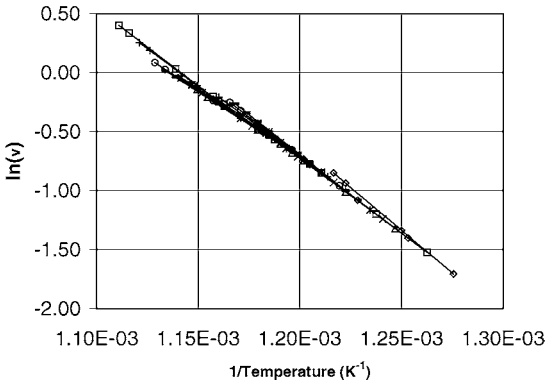

Fig. 7. Differential analysis of non-isothermal data. Arrhenius plot of ln(**v**), i.e. ln(rate) vs. $1/T$ for non-isothermal data for calcite under vacuum (CCVKPM.TXT [6]). The individual plots for the submatrices are superimposed, but only the first and last and two intermediate points are shown for each. Also only every fifth submatrix line is shown for clarity. Various symbols are used for each submatrix.

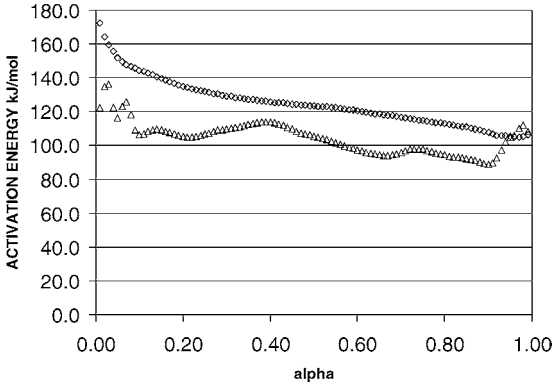

Fig. 8. Variation of activation energy with α for non-isothermal data. Comparison of differential and integral analysis. Non-isothermal data for calcite decomposition under vacuum (CCVKPM.TXT [6]). (△) Differential analysis, (◊) integral analysis.

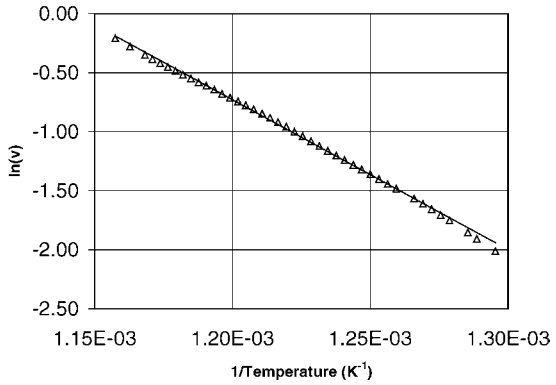

Fig. 9. Differential analysis of non-isothermal data. Arrhenius plot of ln(**v**), i.e. ln(rate) vs. $1/T$ for calcite under vacuum (CCVKPM.TXT [6]). The plot is for the total data after combining all of the **v** values from the submatrices. Only every fifth point is shown for clarity.

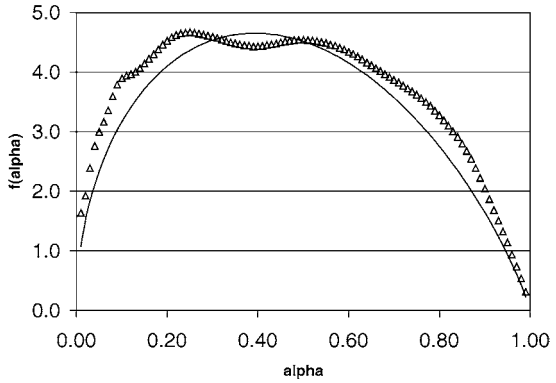

Fig. 10. Differential analysis of non-isothermal data. $f(\alpha)$ vs. α. The data is for calcite decomposition under vacuum (CCVKPM.TXT [6]). The theoretical $f(\alpha)$ are for mechanism A2, i.e. Eq. (13) of Part 1. The experimental and theoretical data are superimposed. (△) Experimental $f(\alpha)$, (—) theoretical $f(\alpha)$ (rescaled data).

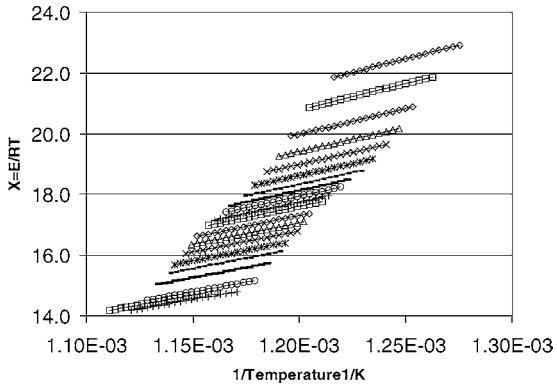

Fig. 11. Integral analysis of non-isothermal data. The data is for calcite under vacuum (CCVKPM.TXT [6]). Superimposed $X = E/RT$ vs. $1/T$ plots for individual submatrices. The plots for the submatrices are superimposed, but only every fifth submatrix is shown for clarity. Various symbols are used for each submatrix.

5.2. Non-isothermal data by an integral analysis

When this analysis was applied to the same data as in Section 5.1, the individual X versus $1/T$ plots produced are shown in Fig. 11.

The lower line shows superimposed symbols showing rapid convergence to the final line. Not all of the symbols are drawn at each $1/T$ point to make the plot clearer leading to a variation in E also shown in Fig. 8. There is much less fluctuation compared to the differential analysis. The combined submatrices produced (Fig. 12) and show the outer iteration as defined in Fig. 1. Again many points are superimposed after the first two lines, because of the rapid convergence. When the plot in Fig. 13 was made of $g(\alpha)$ versus α, the fit of the experimental data to any single mechanism was difficult, but the nearest seemed to be again A2, Eq. (13) of Part 1. The random variations or loops in the plot had gone and there was fair agreement, except perhaps at the highest values of α.

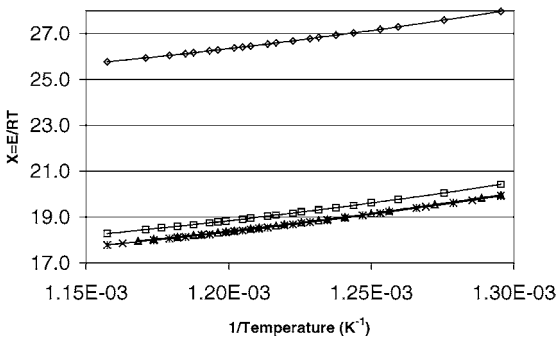

Fig. 12. Integral analysis of non-isothermal data. The data is for calcite under vacuum (CCVKPM.TXT [6]). Combined **v** results from all of the submatrices used in the iterative process. (◊) First step of the iteration, (□) second step of the iteration, (△) third step of the iteration, (×) fourth step of the iteration, (*) fifth step of the iteration.

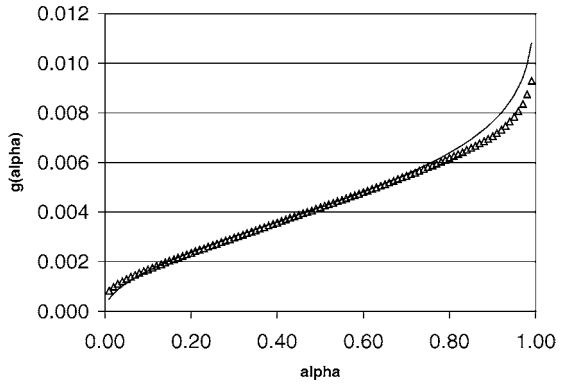

Fig. 13. Integral analysis of non-isothermal data. $g(\alpha)$ vs. α. The data is for calcite under vacuum (CCVKPM.TXT [6]). The theoretical $g(\alpha)$ are for mechanism A2, i.e. Eq. (13) of Part 1. The experimental and theoretical data are superimposed. (△) Experimental $g(\alpha)$, (—) theoretical $g(\alpha)$ (rescaled data).

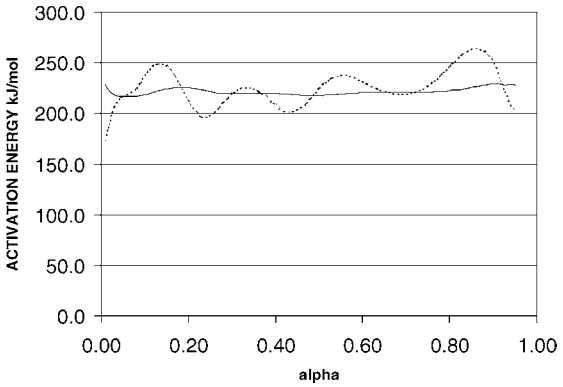

Fig. 14. Analysis of isothermal data for calcite under vacuum (CCVISO.TXT [6] as used in Part 1 of this study). The data is divided into groups of five lines taken from the data matrix **M** and treated to SVD individually, leading to a plot of the individual values of activation energy against α. The differential and integral results are compared. (—) Integral analysis, (- - -) differential analysis.

6. Conclusions

Table 1 shows, as in Part 1, that for simulated data the methods described retrieve the values of E and A with reasonable precision. In this case, differential and integral analysis methods give much the same precision. Identification of the correct kinetic equation was again clear for the simulated data.

For experimental data, a main point of interest is in identifying the equation obeyed. These papers are intended to cover the mathematics of the methods and not to be a study of possible mechanisms. For this reason, attempts are only made to fit the standard equations for known mechanisms. No attempt is made to fit with non-standard exponents because this has been covered elsewhere [6,9–12]. Figs. 7 and 8 of Part 1 show that it is not easy to fit a kinetic equation for fluctuating data. However, Fig. 9 of Part 1 for integral analysis, makes the decision much easier. Comparing Figs. 10 and 13 of Part 2 shows the same point.

The four methods of calculation, described in Parts 1 and 2, lead to single overall values of activation energy. The mechanism may change during the experiments, as α changes, as does temperature. It is too simplistic to just declare one value for E without investigating a change in E over the set of experiments. The non-isothermal data had to be split into submatrices, so the opportunity was taken to calculate E for each submatrix and to plot the results against α. There was no need to divide up the isothermal data in a similar manner, but it was decided that variation in E should also be investigated here. The data could be treated as an isoconversional set and a value of E obtained for each line across the data, i.e. constant α. It was thought more appropriate to use the SVD method, because this would give a degree of smoothing over a set of five lines, as for the non-isothermal case. Since the non-isothermal data was divided into steps of standard α values, five lines at a time, the same was done for the isothermal data. The result, when differential and integral analysis are used, is compared in Fig. 14. Differential analysis shows a great deal of fluctuation and there is not much point in quoting a single overall value for E. Integral analysis shows an almost constant E, so it may be reasonable to quote a single overall value.

A similar comparison may be made for non-isothermal results from SVD in Fig. 8.

These results show that integral analysis is the preferred method. Even the result for simulated data, treated to differential analysis, shows some fluctuation at high α (Fig. 3). It has been suggested by Burnham [10] that these oscillations, in the calcite experiments, may be due to fluctuation in the temperature control system of the apparatus used to produce the data and not to fluctuations in mechanism. This may be true for isothermal data, but since a similar effect is seen for rising temperatures, slight changes in mechanism must at least be suspected. In Fig. 8, the integral analysis shows a definitely decreasing value of E, so quoting a single value for E is pointless, except perhaps when calculation methods are being compared [6]. The values of E differ greatly between isothermal and non-isothermal, but should agree unless mass and heat transfer effects are present or there is a change in mechanism. Maciejewski [9] has pointed out that the ICTAC study isothermal data covers a temperature range of only 35 °C, but the non-isothermal a range of 193 °C, which will lead to opportunity for a change in mechanism in the second case. It may also be noted that the isothermal data cover a range from 515 to 550 °C. The starting temperatures quoted for the set of non-isothermal data cover the range 496–545 °C. Thus the non-isothermal experiments only just reach into the isothermal range. Fig. 8 shows a value of activation energy rising towards lower α values. The value did not reach the isothermal level, but it might if the calculation had continued to lower α values, which would imply lower temperatures for the experiment. Unfortunately the lowest value for α given in the data tables was for 0.01, so the calculation could not be continued to lower values of α. Examining only the integral results for fitting a mechanism, there is a closer fit for the isothermal

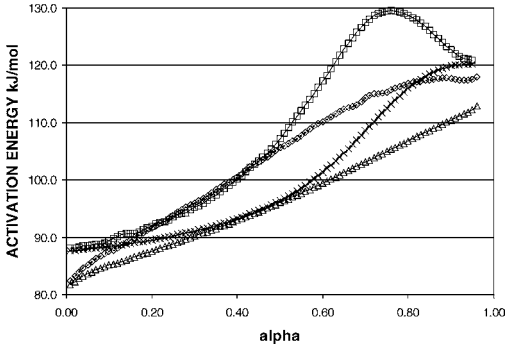

Fig. 15. Variation of activation energy with α for differential and integral analysis, isothermal and non-isothermal data. Simulated data for two simultaneous first order reactions (SIMISO.TXT and SIMKPM.TXT from Ref. [6]). (◊) Non-isothermal data, differential analysis, (△) non-isothermal data, integral analysis, (□) isothermal data, differential analysis, (×) isothermal data, integral analysis.

result (Fig. 9, Part 1) than non-isothermal (Fig. 13, Part 2). This suggests again a mechanism change in the second case. The results for these sample data, which appear in tables in Ref. [6], show a wide range of variability according to the methods employed and the workers carrying out the calculation. However, the present results for non-isothermal decomposition of calcite under vacuum agree with the result by Nomen and Sempere (SVD method), in that paper, in respect to the value of E, but not of A. The results for the isothermal data are more consistent in Ref. [6] and agree mostly with the results obtained here.

It has been suggested that the use of integral methods may introduce systematic errors into resulting values of activation energies. This may be true for overall activation energies produced by combining all of the data from the experiment into one SVD step. However, as shown above, the activation energy may vary during decomposition and it is better to use the results of separate submatrices and to show the variation. In the present study each submatrix contained five lines of data, so any error introduced would be restricted to only a small range of time or temperature. The ICTAC study [6] also included simulated data for two simultaneous, equally weighted, first order reactions. They were given activation energies E_1 = 80 kJ mol^{-1}, E_2=120 kJ mol^{-1} and pre-exponential factors of A_1=10^{10} min^{-1}, A_2=10^{15} min^{-1}. Vyasovkin [12] has presented an analysis of the results produced by the many workers taking part in the project and using several different methods of calculation. The methods detailed in the present two papers were applied to the same data and the results are summarised in Fig. 15. These may be compared to Fig. 3 in Vyasovkin's paper. The integral results for both isothermal and non-isothermal data seem to be very close to the results produced by Vyasovkin's own method, which is essentially integral in nature. The shapes of the plot of activation energy versus α also agree with the shapes forecast by Vyasovkin in his Figs. 1 and 2 [12]. The corresponding differential analysis of isothermal data produced a curve that went up to a peak of 130 kJ mol^{-1}, i.e. well above the maximum possible of 120 kJ mol^{-1}. Vyasovkin, in his Fig. 3 for some other differential methods, also saw this. As he points out, this must be faulty and is an artefact of the calculation. The differential analysis of non-isothermal data gives results that correctly lie all between 80 and 120 kJ mol^{-1}. However the curve rises rather too steeply and turns to near horizontal near to α = 1. The shape is not as forecast by Vyasovkin in his Fig. 2. Thus it is the differential methods that are suspect, not the integral ones. Vyasovkin [12] also comments on the process of numerical differentiation of original data leading to erroneous values of activation energy as suggested here ([8,9] in Part 1).

There are many other methods of analysis available for these types of data, especially for the isothermal experiments, see [6]. A recent paper [13] has proposed combined kinetic analysis allowing simultaneous analysis of experiments obtained under any heating profile. It may be possible to apply data from other heating profiles to the NPK method if the data from the individual submatrices can be combined into a single matrix.

NPK analysis is of importance, as discussed by Sewry and Brown [5]. These papers have shown that data may be best analysed by integral analysis, but a differential technique appears to give a more variable result.

Acknowledgement

Professor Michael Brown of Rhodes University, Grahamstown, South Africa, kindly supplied the data from the ICTAC kinetic study [6].

References

[1] J. Sempere, R. Nomen, R. Serra, Thermochim. Acta 316 (1998) 37–45.
[2] J. Sempere, R. Nomen, R. Serra, J. Therm. Anal. Calorimetry 52 (1998) 933–943.
[3] J. Sempere, R. Nomen, R. Serra, J. Therm. Anal. Calorimetry 56 (1999) 843–849.
[4] J. Sempere, R. Nomen, R. Serra, J. Soravilla, Thermochim. Acta 388 (2002) 407–414.
[5] J.D. Sewry, M.E. Brown, Thermochim. Acta 390 (2002) 217–225.
[6] M.E. Brown, M. Maciejewski, S. Vyasovkin, R. Nomen, J. Sempere, A. Burnham, J. Opfermann, R. Strey, H.L. Anderson, A. Kremmler, R. Keuleers, J. Janssens, H.O. Desseyn, C.-R. Li, T.B. Tang, B. Roduit, J. Malek, T. Mitsuhashi, Thermochim. Acta 355 (2000) 125–143.
[7] G.R. Heal, Thermochim. Acta 340/341 (1999) 69–76.
[8] J.H. Flynn, Thermochim. Acta 300 (1977) 83–92.
[9] M. Maciejewski, Thermochim. Acta 355 (2000) 145–154.
[10] A.K. Burnham, Thermochim. Acta 355 (2000) 165–170.
[11] B. Roduit, Thermochim. Acta 355 (2000) 171–180.
[12] S. Vyasovkin, Thermochim. Acta 355 (2000) 155–163.
[13] L.A. Pérez-Maqueda, J.M. Criado, F.J. Gotor, J. Málek, J. Phys. Chem. A 106 (2002) 2862–2868.